Food Chemistry 343 (2021) 128473

Contents lists available at ScienceDirect

Food Chemistry

journal homepage: www.elsevier.com/locate/foodchem

Predicting micronutrients of wheat using hyperspectral imaging

Naiyue Hu [a,1], Wei Li [a,1], Chenghang Du [a], Zhen Zhang [a], Yanmei Gao [a], Zhencai Sun [a,b], Li Yang [c], Kang Yu [a,b,d,*], Yinghua Zhang [a,b,*], Zhimin Wang [a,b,*]

[a] College of Agronomy and Biotechnology, China Agricultural University, Beijing 100193, China
[b] Engineering Technology Research Center for Agriculture in Low Plain Areas, Heibei Province, China
[c] College of Engineering, China Agricultural University, Beijing 100193, China
[d] School of Life Sciences, Technical University of Munich, Freising 85354, Germany

ARTICLE INFO

Keywords:
Wheat grain
Grain nutritional attribute
Wheat flour
PLSR
Grain quality
Visible and near-infrared reflectance spectroscopy

ABSTRACT

Micronutrients are the key factors to evaluate the nutritional quality of wheat. However, measuring micronutrients is time-consuming and expensive. In this study, the potential of hyperspectral imaging for predicting wheat micronutrient content was investigated. The spectral reflectance of wheat kernels and flour was acquired in the visible and near-infrared range (VIS-NIR, 375–1050 nm). Afterwards, wheat micronutrient contents were measured and their associations with the spectra were modeled. Results showed that the models based on the spectral reflectance of wheat kernel achieved good predictions for Ca, Mg, Mo and Zn ($r^2 > 0.70$). The models based on the spectra reflectance of wheat flour showed good predictive capabilities for Mg, Mo and Zn ($r^2 > 0.60$). The prediction accuracy was higher for wheat kernels than for the flour. This study showed the feasibility of hyperspectral imaging as a non-invasive, non-destructive tool to predict micronutrients of wheat.

1. Introduction

Being a major staple food crop, wheat provides about 20% of the total dietary calories and proteins worldwide (Shiferaw et al., 2013). Wheat also contains several other essential nutrients, including dietary fiber, lipids, micronutrients and phytochemicals, which contribute to human health (Shewry, 2009). Although wheat contains a variety of nutrients, it cannot meet the nutritional needs of the human body when people are only relying on wheat as the major source of nutrition. Thus, the problem of "Hidden Hunger" is particularly acute in some developing countries where wheat is the staple food (Gómez-Galera et al., 2010). The World Health Organization (WHO) defines "Hidden Hunger" as an inadequate or unbalanced intake of nutrients. The Copenhagen Consensus listed micronutrient deficiencies as the fifth biggest global challenge to human health in 2008. It is estimated that 2 billion people worldwide suffer from one or more chronic micronutrient deficiencies (Kumssa et al., 2015), and China accounts for 15% of the total. Therefore, it is crucial to evaluate and improve the nutritional quality of wheat in the context of global food and nutrition security.

Biofortification through wheat breeding is one of the primary ways to improve the nutritional quality of wheat (Rawat, Neelam, Tiwari, & Dhaliwal, 2013). However, screening a large amount of wheat germplasms needs plenty of laboratory-based measurements of wheat nutritional and quality parameters, including micronutrient measurements. Micronutrients, such as boron (B), calcium (Ca), copper (Cu), iron (Fe), magnesium (Mg), manganese (Mn), molybdenum (Mo) and zinc (Zn), are essential nutrients which the human body needs in small quantities (Bouis & Welch, 2010). Traditional chemical methods for the determination of micronutrient contents have high accuracy, but they have some disadvantages, such as they are time-consuming, laborious, expensive and contribute to environmental contamination. In addition, the traditional chemical methods cannot complete the micronutrient determination of large numbers of wheat germplasms economically and quickly, which limits the applicability in breeding programs. Therefore, it is necessary to develop a high-throughput and economical method for the determination of micronutrients in wheat.

Near-infrared (NIR) spectroscopy has been increasingly used for kernel quality measurements, such as wheat moisture content (Peiris &

* Corresponding authors at: College of Agronomy and Biotechnology, China Agricultural University, Yuanmingyuan West Road No.2, Beijing 100193, PR China.
E-mail addresses: 13598600759@163.com (N. Hu), wellion@cau.edu.cn (W. Li), duchenghang0726@163.com (C. Du), zhangsirzz@163.com (Z. Zhang), 18235409700@163.com (Y. Gao), zhencai_sun@cau.edu.cn (Z. Sun), yangli@cau.edu.cn (L. Yang), kangyu@cau.edu.cn (K. Yu), zhangyh1216@126.com (Y. Zhang), zhimin206@263.net (Z. Wang).
[1] These authors contributed equally to this work.

https://doi.org/10.1016/j.foodchem.2020.128473
Received 7 May 2020; Received in revised form 28 September 2020; Accepted 21 October 2020
Available online 26 October 2020

Dowell, 2011), protein content (Shi, Lei, Louzada Prates, & Yu, 2019), gluten protein content (Cai, 2017) and amylose content (Delwiche, Graybosch, Amand, & Bai, 2011). NIR spectroscopy allows to characterize sample constituents using spectra from the 'point-source' measurements, but usually, it lacks the visible spectral region and spatially-explicit spectral variations that might be useful for determining minor components (Gowen et al., 2007). Therefore, NIR spectroscopy cannot fully capture the gradient of internal compositions in samples. Hyperspectral imaging (HSI) is a new technique that integrates conventional spectroscopy and imaging to capture both spatial and spectral characteristics of samples (Gowen et al., 2007). Although HSI was originally developed for remote sensing, it has become a high-throughput non-destructive tool for grain sample analysis. HSI has been successfully applied to measure the cereal quality attributes, such as wheat kernel hardness (Mahesh, Jayas, Paliwal, & White, 2015), water content (Zheng et al., 2016) and protein content (Caporaso, Whitworth, & Fisk, 2018a; Mahesh et al., 2015). Also, HSI has been applied to measure the cereal safety attributes, such as *Fusarium* infection and mycotoxin contamination (Alisaac et al., 2019), sprouting detection (Xing et al., 2009) and parasitic contamination (Singh, Jayas, Paliwal, & White, 2009). However, the potential of HSI technology for measuring cereal multiple micronutrients is still underexplored.

The distribution of micronutrients in wheat kernels is uneven, and most of the micronutrients are mainly located in the seed coat and aleurone layer (Persson et al., 2016). HSI technology increases the spatial dimension and can obtain spectral information of each pixel in the image, which is promising for analyzing samples of heterogeneous nature (Manley, 2014). Micronutrients (e.g., Ca, Mg, B, Cu, Fe, Mn, Mo and Zn) are not spectrally active compounds, and they do not produce active spectral absorption characteristics in the VIS-NIR region (Pandey, Ge, Stoerger, & Schnable, 2017). Instead, these micronutrients can be indirectly measured by co-variation with the organic components in the kernel (Manley, 2014). For example, Zn is associated with gliadin, glutenin, albumin and globulin concentrations in wheat kernels (Liu, Wang, Rengel, & Zhao, 2015). Persson et al. (2016) also demonstrated the presence of zinc-binding proteins and zinc-containing enzymes in wheat endosperm. However, to which extent the different micronutrients can be predicted using HSI requires further investigations.

The morphological differences of samples may affect the use of spectral reflectance for the prediction of sample constituents. It has been shown that the spectral signature of wheat kernels is different from flour produced from these kernels (Alisaac et al., 2019; Delwiche, Graybosch, Amand, & Bai, 2011). Therefore, the predictions may be different between using the spectral reflectance of kernel and flour. In addition, the information related to the natural variability of individual samples can be reduced when using ground samples, as grinding produces a relative homogeneous material for the spectral imaging camera (Caporaso, Whitworth, & Fisk, 2018b). It is argued that better predictions can be obtained by using the spectral data resulted from measuring the ground samples compared to measuring the whole kernels (Caporaso, Whitworth, & Fisk, 2018b). Yet, grinding samples is still a time-consuming procedure that slows down the entire measurement pipeline when a large number of samples need to be measured. If the prediction results based on the spectral reflectance of the kernel are not significantly different from that based on the spectral reflectance of ground sample, kernel spectral measurements will bring new opportunities to the rapid determination of micronutrients in grains. Therefore, the difference between using wheat kernel and flour samples for the spectroscopic prediction of micronutrient contents need to be further investigated.

In this study, we proposed an economical approach for rapid determination of micronutrients in wheat grains using HSI, and we hypothesized that grain micronutrients can be predicted by directly imaging the intact kernels. Accordingly, our objectives were 1) to evaluate the feasibility of using HSI to estimate wheat micronutrient, including the B, Ca, Cu, Fe, Mg, Mn, Mo and Zn; and 2) to evaluate whether micronutrient contents of wheat could be predicted directly from the hyperspectral reflectance of the wheat kernel, without destructive preprocessing of kernel samples into flour.

2. Materials and methods

2.1. Site description, wheat sample collection

The field experiments were implemented at Wuqiao Experimental Station of China Agricultural University (Hebei Province, China; 116.3°E, 37.4°N; altitude: 20 m) in 2017–2019. Across years and sites, different agronomical management practices and genotypes were used in eight experiments to reflect a gradient in the micronutrient content in wheat kernels (Table S1). Rainfall and temperature during the two growing seasons are shown in Fig. S1. Thirteen wheat cultivars were used in the study (Table S1, Table S2), i.e. the Beijing 8, Fengkang 8, Nongda 139, Jing 411, and nine cultivars currently still cultivated in China (Gaoyou 2018, Gaoyou 5766, Hanmai 15, Jimai 22, Nongda 399, Shimai 22, Zhongmai 1062, Zhongmai 175 and Zhongmai 578). A total of 631 samples of wheat kernels were collected at complete maturity. The information of the specific source for wheat samples is shown in Table S1. After wheat kernel samples were naturally air-dried, hyperspectral images were acquired. Then the wheat kernel samples were washed five times with deionized water, and dried at 70℃ to constant weight, ground with a ball mill using the zirconia grinding tank. The hyperspectral image of wheat flour samples was also collected by HSI and then chemically analyzed for micronutrient contents.

2.2. Hyperspectral imaging process

In this experiment, an HSI system was used to collect the spectral image of samples. The HSI system consists of a hyperspectral imager, a dark box, a lighting system, a lifting platform and a computer (Fig. 1a). The portable VIS-NIR hyperspectral imager SOC710-VP (Surface Optics Corporation, USA) was used to acquire the spectral images. It covers the spectral range from 375 to 1050 nm at 5 nm increments for a total of 128 bands, with an image resolution of 690 × 520 pixels. The experiment was performed in a dark box in order to reduce the effect of natural light. The lighting system consists of four halogen lamps (60 W) around the top of the dark box. The wheat kernel (20–25 g) or flour (7–10 g, ~ 1 cm

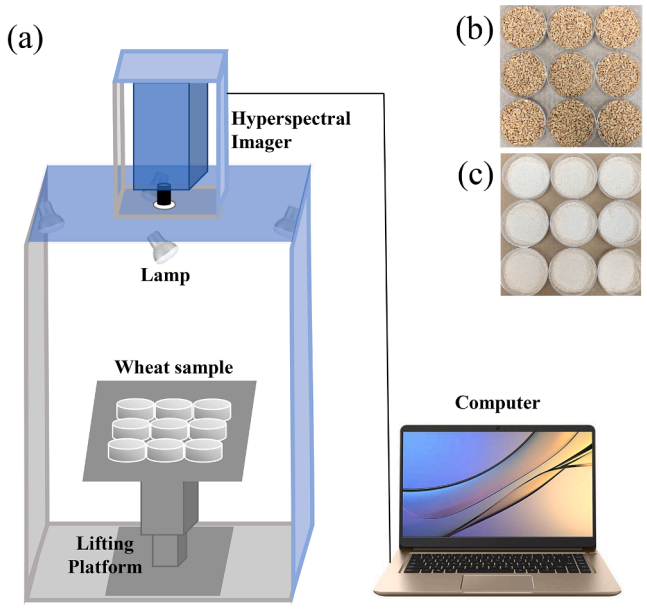

Fig. 1. Hyperspectral imaging acquisition system. The HSI system (a) consists of a hyperspectral imager, a dark box, a lighting system, a lifting platform and a computer. (b) Wheat kernel sample, (c) wheat flour sample.

depth) samples were put in a plastic box (6 cm in diameter, 2 cm in height) and placed on the lifting platform. Before imaging, the flour was pressed to be flattened with plastics (prevent metal contamination). The spectral reflectance of 9 samples were captured at the same time (Fig. 1b, c). Images were captured and saved to the computer using the HyperScanner2.0 software. During this process, the gray reference panel of known reflectance was placed in the same imaging area as the sample. All images were collected under the same conditions. Raw images were corrected for dark-offset based on the dark current recorded in each image. Afterwards, the gray reference panel in each raw image was used to perform the radiometric calibration, and then a reflectance image was obtained. After converting the raw spectral radiance image into a spectral reflectance image, the average reflectance of the region of interest (ROI) for each sample was extracted from the image by using Spectral Radiance Analysis Software (Surface Optics Corporation, USA). When selecting the ROI, the shadows and highlights in the image were excluded.

2.3. Determination of wheat kernel micronutrient content

Micronutrient content measured from wheat flour, 0.2 ~ 0.3 g (accurate to 0.0001 g) sample was placed in a microwave digestion tank, then added 2:1 HNO_3:H_2O_2 acid mixture and standing for 12 h. After standing, the sample was digested by the microwave digestion apparatus (CEM Mars6, USA). Digested solution of the sample was transferred to a 25 ml volumetric flask, added up deionized water to dilute to graduation, shaken up evenly and then filtered with a 0.45 μm filter membrane. Filter liquor was analyzed for B, Ca, Cu, Fe, Mg, Mn, Mo and Zn using the Inductively coupled Plasma Atomic Emission Spectrometer (Thermo-ICAP6300, USA).

2.4. Modeling

Before modeling, the outliers from the measured micronutrients dataset were identified and removed using the Tukey's rule (Coast et al., 2019), and hyperspectral outliers were detected and removed using a Monte Carlo cross-validation based method (Liu, Cai, & Shao, 2008). The outlier removal was performed independently for each dataset for micronutrient, and the kernel- and flour-spectral data. Details of the sample number removed are shown in Table S3. The final number of observations for each element prediction model ranges from 489 to 567 and 485 to 563 for wheat kernel and flour, respectively. In accordance with the principle of maintaining the uniform distribution of each wheat cultivar in each subset, the measured micronutrients data were divided into two datasets: (1) a calibration data set with 80% of the observations; (2) a validation data set comprising the remaining 20% observations. The balanced split function create Data Partition in the "caret" package was used to maintain an even distribution of wheat cultivar in calibration and validation subset (Kuhn, 2015). This technique performs the random sampling within each wheat cultivar and would preserve the same cultivar distribution of calibration and validation data to overall data.

The spectral preprocessing, such as 1st derivative (FD), 2nd derivative (SD), constant offset elimination (COE), vector normalization (VN), min–max normalization (MMN) and multiplicative scatter correction (MSC), was used to screen the model with the highest accuracy.

Partial least squares regression (PLSR) was used to model the spectra and nutrient trait relationships (Atzberger, Guérif, Baret, & Werner, 2010). Spectral wavelengths of 375–1050 nm were used for all element predictions. Model was created for each nutrient element, the performance of each model was evaluated using the coefficient of determination (r^2), root mean square error (RMSE) and regression bias (Reg. bias) of prediction from the validation dataset. To quantify the difference in predictive performance between the two materials, the difference between the wheat kernel and wheat flour divided by the wheat flour was defined as the variation amplitude. The predictive power was classified according to Ely et al. (2019) and Coast et al. (2019). The predictive capability of the model was considered as, i) very high when $r^2 > 0.85$, ii) good when $0.85 > r^2 > 0.60$, iii) medium when $0.60 > r^2 > 0.50$, and iv) poor when $r^2 < 0.50$. The relative contribution of each wavelength to the PLSR model was evaluated using the variable importance of projection (VIP) (Ely et al., 2019). Wavelength selection based on VIP result (the wavelength of VIP > 0.8 was selected) was used to screen the model with higher accuracy. PLSR models were implemented with the "pls" package in the R software (R Core Team, 2019).

3. Results

3.1. Wheat kernel and wheat flour reflectance spectral properties

The spectral reflectance of the wheat kernel (n = 631) and wheat flour (n = 631) were quite different from each other (Fig. 2a and b). Although the spectral reflectance of the wheat kernel and wheat flour both showed a parabola trend with the increased wavelength, the peak of the wheat kernel was lower than wheat flour. The average reflectance of the wheat flour samples was higher than that of the wheat kernel samples. The wheat kernel reflectance showed the largest variations in the near-infrared region (Fig. 2a), while the wheat flour reflectance showed variations in the both visible and near-infrared regions (Fig. 2b).

3.2. Variation in wheat micronutrient content

Descriptive statistics for the micronutrient contents of wheat kernel and flour are shown in Table 1. For the micronutrient data used in the wheat kernel model, B has the highest coefficient of variation (CV = 38.6%), followed by Mo (CV = 24.8%), and the smallest by Mg (CV = 7.8%). The micronutrient data used in the wheat flour model showed the same regularity. In general, the content of wheat nutrients showed a significant variability among the 13 selected cultivars (Fig. S2).

3.3. PLSR prediction model

The prediction results of wheat kernel showed that the models achieved good predictive power for Ca, Mg, Mo and Zn content. In addition, they showed a medium predictive capability for Cu content. While the models had poor predictive capabilities for B, Fe and Mn content (Table 2). The prediction results of wheat flour also showed the models achieved good predictive power for Mg, Mo and Zn content. In addition, they showed a medium predictive capability for Cu content, and had poor predictive capabilities for B, Ca, Fe and Mn content (Table 2).

The prediction for the wheat kernel was comparable to the prediction for the wheat flour (Table 2). The variation amplitude of r^2 for B, Ca and Zn was greater than 10% (Table 2, Fig. 3), which indicates that the r^2 of B, Ca and Zn predicted by the use of wheat kernel spectral reflectance was relatively higher than that predicted by flour. The variation amplitude of RMSE for Ca, Mo and Zn was less than −10% (Table 2, Fig. 3), which indicates that a smaller prediction error for Ca, Mo and Zn was obtained when using wheat kernel spectra than using the flour spectra. Therefore, the prediction power of the wheat kernel models was slightly better than that of wheat flour models.

The VIP is a standard method to identify the most important wavelength region from the PLSR model. The regions of high importance to all element models existed in both visible and NIR regions (Fig. 4). For wheat kernels, 400–450 nm and 850–950 nm showed high importance for all element models, and the peak at 675 nm was important for most elements (Fig. 4A). The VIP curves for the models (B, Fe and Mn) with poor prediction performance showed many small peaks, while the VIP curves for those models (Ca, Mg, Mo and Zn) with good prediction performance showed fewer peaks (Fig. 4A). For wheat flour, 400–425 nm and 850–950 nm showed the high importance for all element models, and the peak at 675 nm was important for B, Ca, Fe, Mn

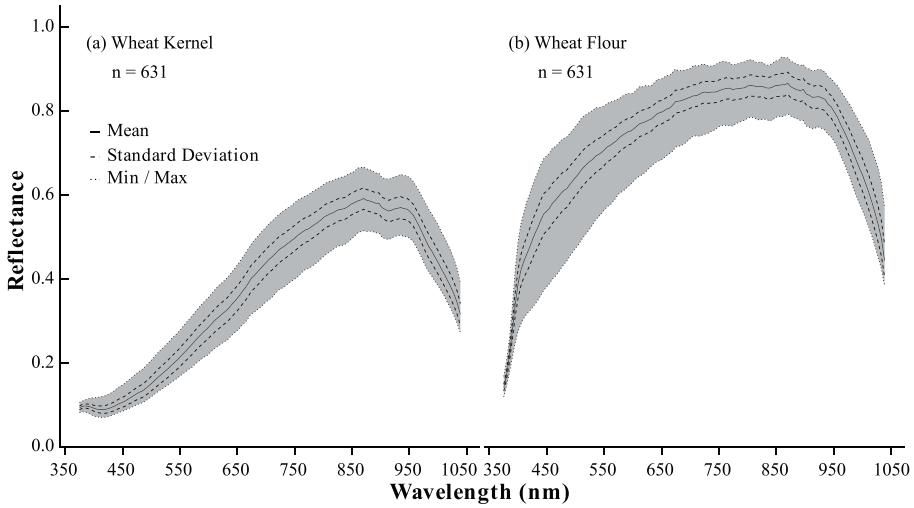

Fig. 2. The mean, ± standard deviation, minimum and maximum spectral reflectance for wheat kernel (a, n = 631) and wheat flour (b, n = 631) samples.

Table 1
Descriptive statistics of the wheat micronutrient contents for the modelling calibration and validation datasets.

Nutrient	Wheat kernel					Wheat flour				
	SN	Mean	Max	Min	CV (%)	SN	Mean	Max	Min	CV (%)
		mg/kg					mg/kg			
B	489	1.18	2.60	0.07	38.6	485	1.21	2.60	0.07	36.7
Ca	544	324	431	222	12.0	544	324	437	222	11.8
Cu	536	4.32	6.81	2.73	19.5	535	4.32	6.70	2.73	19.5
Fe	536	32.02	42.14	23.10	11.1	537	31.96	43.05	24.17	10.9
Mg	564	1458	1796	1226	7.8	563	1463	1796	1213	7.9
Mn	558	31.91	39.28	21.52	8.7	561	31.92	39.71	24.85	8.6
Mo	556	0.80	1.36	0.45	24.8	558	0.82	1.35	0.44	25.0
Zn	567	26.23	41.63	14.66	22.6	563	26.14	41.56	14.66	22.8

SN: sample number; CV: coefficient of variation.

Table 2
Performance comparison of hyperspectral reflectance of wheat kernel and wheat flour to predict wheat nutrient content.

Nutrient	r^2			RMSE (mg/kg)			Reg. Bias (mg/kg)		
	WK	WF	VA	WK	WF	VA	WK	WF	VA
B	0.28	0.21	37%	0.41	0.43	−5%	0.78	0.83	−6%
Ca	0.70	0.48	45%	22.42	28.60	−22%	56.10	161.04	−65%
Cu	0.57	0.59	−4%	0.54	0.55	−3%	1.52	1.72	−12%
Fe	0.34	0.35	−2%	2.86	3.01	−5%	18.48	16.32	13%
Mg	0.74	0.72	2%	60.06	61.01	−2%	287.81	375.54	−23%
Mn	0.34	0.32	5%	2.30	2.20	5%	17.37	16.76	4%
Mo	0.82	0.77	6%	0.08	0.10	−16%	0.08	0.12	−29%
Zn	0.77	0.63	23%	2.90	3.59	−19%	3.75	8.49	−56%

r^2: coefficient of determination; RMSE: root mean square error; Reg. bias: regression bias; WK: wheat kernel; WF: wheat flour; VA: variation amplitude, defined as the difference between wheat kernel and wheat flour divided by the wheat flour.

and Zn (Fig. 4B). The VIP results of wheat flour also revealed a certain correlation between the smoothness of VIP curves and the model performance. The VIP curves had more peaks of the model with poor prediction performance, such as B, Ca, Fe and Mn (Fig. 4B). The VIP curves for the wheat kernel model show fewer peaks than the wheat flour model.

The r^2 of the PLSR model using six spectral preprocessing techniques and the VIP-based wavelength selection is shown in Table S4. The difference range of r^2 was −0.28–0.03 for wheat kernel and −0.24–0.04 for wheat flour between using raw data and using spectral preprocessing or wavelength selection. Therefore, the prediction accuracy of the PLSR model was not significantly improved when applying the spectral preprocessing or VIP-based wavelength selection.

4. Discussion

A large data set of wheat micronutrient contents (631 samples) from 13 wheat cultivars under different environmental conditions and agronomical management practices were presented in this study. And this study has demonstrated the capability of non-destructive prediction of wheat micronutrient contents using wheat kernel imaging spectroscopy.

4.1. Variation in wheat micronutrients

A large variation (CV > 10%) in B, Ca, Cu, Fe, Mo and Zn was observed in this study. Similarly, a previous study found that the CV of Ca, Cu, Fe, Mn and Zn in 265 Chinese wheat cultivars was greater than

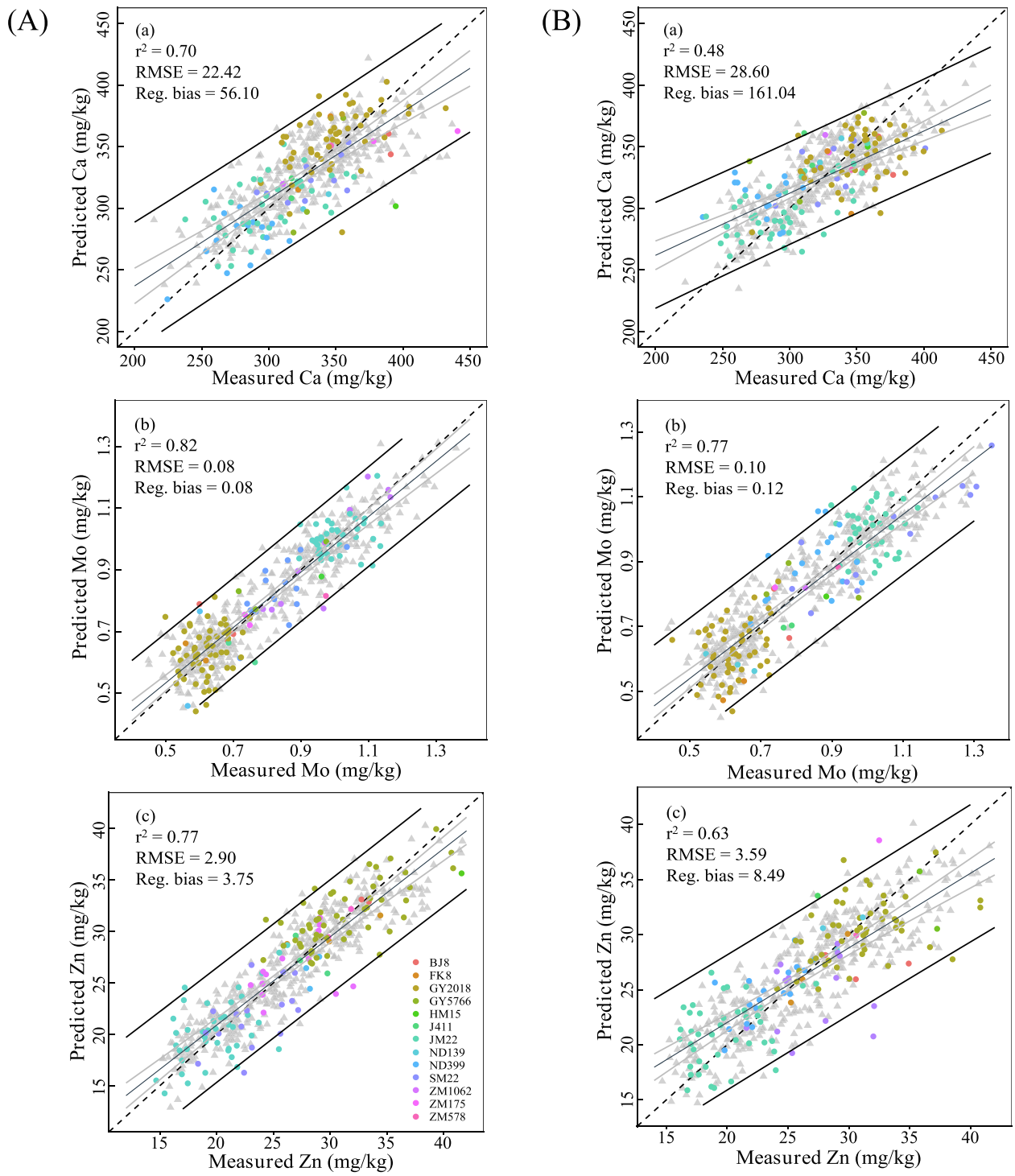

Fig. 3. Results for PLSR models of, Ca (a), Mo (b) and Zn (c) content (mg/kg) using hyperspectral reflectance of wheat kernel (A) and wheat flour (B). Calibration (gray triangles) and validation (color circles) data points are shown. 95% prediction interval (black lines), 95% confidence interval (grey lines), regression line (fine black line) and 1:1 line (dashed line) are shown. BJ8: Beijing 8, FK8: Fengkang 8, GY2018: Gaoyou 2018, GY5766: Gaoyou 5766, HM15: Hanmai 15, J411: Jing 411, JM22: Jimai 22, ND139: Nongda 139, ND399: Nongda 399, SM22: Shimai 22, ZM1062: Zhongmai 1062, ZM175: Zhongmai 175 and ZM578: Zhongmai 578.

10% (Zhang et al., 2010). Although only 13 wheat cultivars were used in this study, the CV of Cu and Zn (19.5% and 22.6%) in this study was greater than the CV of Cu and Zn (12.0% and 14.6%) in the 265-cultivars study (Zhang et al., 2010). Previous studies have also shown that Cu and Zn content could be affected pronouncedly by the growing environments and nitrogen management (Zhang et al., 2010; Hamnér, Weih, Eriksson, & Kirchmann, 2017), which suggests that the observed large variations in Cu and Zn contents might be influenced by the varied environments conditions (multiple years and sites) and agronomical managements in this study.

4.2. *Performance of predicting wheat micronutrients using hyperspectral imaging*

Previous leaf-level studies showed that Ca ($r^2 = 0.70$), Cu ($r^2 = 0.86$), Fe ($r^2 = 0.68$), Mg ($r^2 = 0.69$), Mn ($r^2 = 0.64$) and Zn ($r^2 = 0.73$) in maize

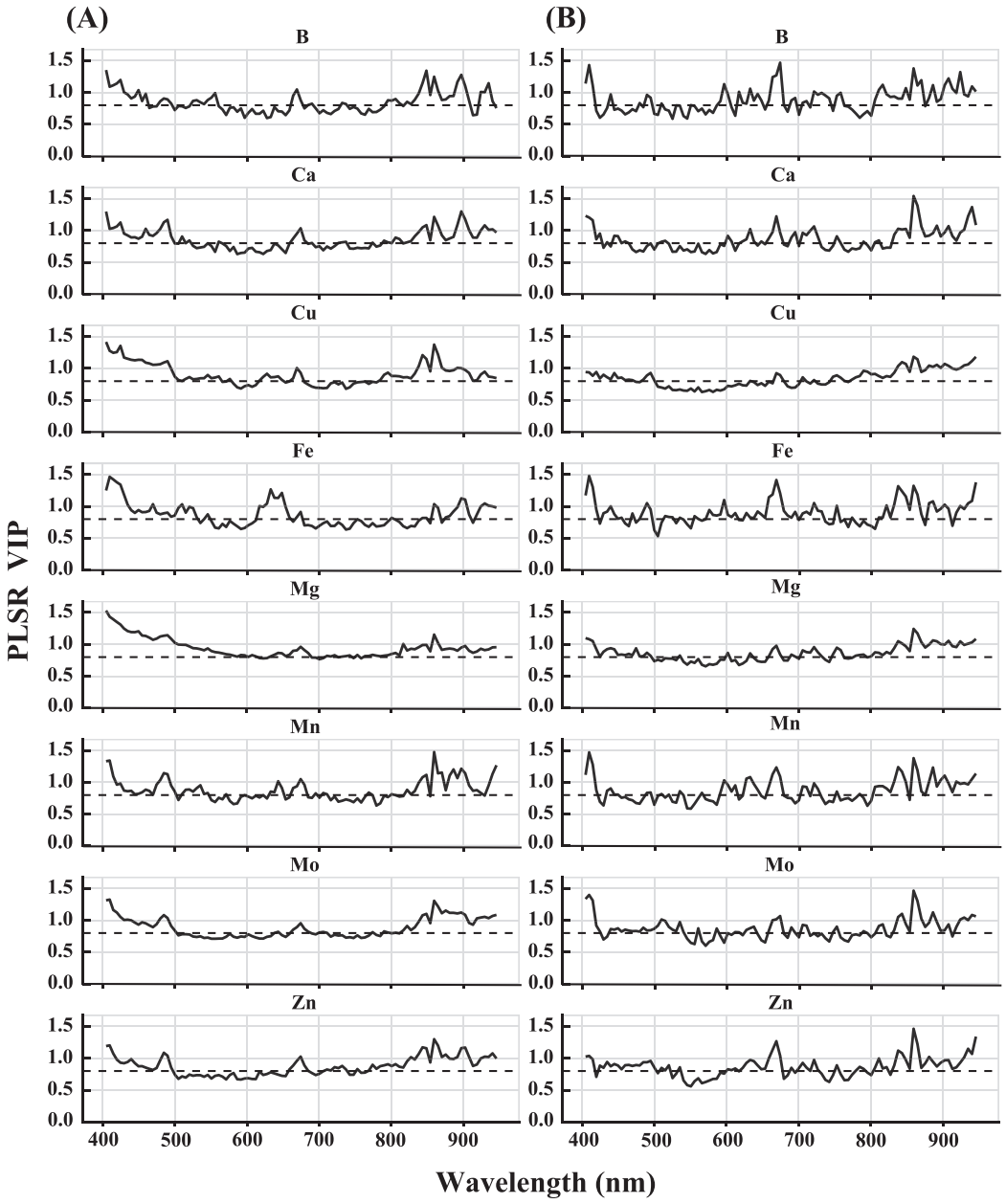

Fig. 4. PLSR model variable importance of projection (VIP) of wheat kernel (A) and wheat flour (B) for B, Ca, Cu, Fe, Mg, Mn, Mo and Zn contents (mg/kg). VIP values of 0.8 (dashed line) is shown.

and soybean leaves can be successfully predicted using leaf spectra in the spectral region of 550–1700 nm (Pandey et al., 2017). In addition, micronutrients of the grain had been well characterized and estimated by HSI (Wiegmann et al., 2019), and the results showed that Fe ($r^2 = 0.64$), Mg ($r^2 = 0.81$) and Zn ($r^2 = 0.71$) in barley grain can be successfully predicted using kernel spectra in the spectral region of 970–2500 nm. In contrast, this study failed to predict Fe ($r^2 = 0.34$) and Mn ($r^2 = 0.34$) in wheat kernels. This might be attributed to the fact that the value ranges of Fe and Mn contents in this experiment were relatively small compared to Pandey, Ge, Stoerger, & Schnable (2017) and Wiegmann et al. (2019). Although the content of Mo was very low, a good predictive ability for Mo was found for the first time using HSI. The relatively large variation (CV = 24.8%) in Mo content might explain the high prediction performance.

Spectral preprocessing and wavelength selection can improve the accuracy of prediction (Wu & Sun, 2013; Sendin, Williams, & Manley, 2017). Spectral data preprocessing is an important step of chemometrics modeling, which is designed to correct the effects from random noise, light scattering and length variation of the light path to improve the performance of models (Wu & Sun, 2013). Most of the preprocessing steps can reduce the spectral- and spatial resolutions, but, preprocessing should only be applied when it is beneficial (Wu & Sun, 2013; Sendin, Williams, & Manley, 2017). Malmir et al. (2019) have shown that the orthogonal signal correction, standard normal variate, number of latent variables and multiplicative scatter correction could increase the accuracy of PLSR models. It has also been reported by Tamburini et al. (2017) that the full-multiplicative scatter correction, standard normal variate, the 1st and 2nd derivatives could increase the accuracy of the PLSR models. In contrast, Caporaso, Whitworth, & Fisk (2018a) showed that there was no improvement in the accuracy of models when applying the multiplicative scatter correction, standard normal variate, 1st or 2nd derivatives, which was similar to the results observed in this study.

Wavelength selection can reduce the collinearity between contiguous wavelengths and eliminate irrelevant information (Wu & Sun,

2013). It allows the transforming of the whole hyperspectral data cube into a reduced dimension, speeding up the data processing and improving the accuracy of the prediction results (Wu & Sun, 2013). However, as also observed in this study, the difference between using the full wavelengths and using the VIP-based wavelengths might be negligible (Bai et al., 2018).

4.3. Comparison between predicting models of wheat kernel and flour samples

Interestingly, the prediction of B, Ca, Mg, Mn, Mo and Zn was superior based on the kernel spectra compared to the use of the flour spectra in this study. The difference in prediction accuracy between the prediction models of wheat kernel and flour samples could be explained in the following three aspects. Firstly, grinding kernels to flour samples could lead to an increase in spectral reflectance across all wavelengths, which might affect the prediction accuracy. Secondly, the content of micronutrients in wheat was relatively low, and most of them were concentrated in the aleurone layer (Brier et al., 2016). The Cu, Fe, Zn, Mg and Mo are mainly distributed at 30–85 μm from the edge of the grain, which corresponds to the aleurone layer, and Mn, Ca and B are mainly distributed at 20–50 μm (Wu et al., 2013; Brier et al., 2015, 2016). The spectral signals can convey information of the sample components in wheat flour by detecting into a depth of approximately 1.8 mm (Laborde et al., 2020). Accordingly, HSI may have the ability to sense the nutrient variations in the aleurone layer of wheat kernels. Therefore, using kernel reflectance resulted in better predictions for B, Ca, Mg, Mn, Mo and Zn than using the flour reflectance data. And thirdly, kernel grinding generally dilutes micronutrients in the samples, which could have resulted in a poor prediction for B, Ca, Mg, Mn, Mo and Zn using flour spectra in this study. However, compared to the models based on flour spectra, models using kernel spectra did not improve the prediction accuracy for Fe and Cu. The subtle difference between the spectral predictions for individual micronutrients and the underlying mechanisms explaining the subtle difference still need further investigations in future.

4.4. Important spectral regions for predicting wheat micronutrient content

The VIP curves reveal the important spectral regions of predicting each wheat nutrient element. In this study, the important spectral regions of wheat nutrient elements were 400–450 nm, 650–695 nm and 850–950 nm, overlapping with the important wavelengths reported by Bai et al. (2018) for predicting mineral nutrition in edible tree nuts. For example, the spectral regions of 400 nm, 670–690 nm and 800–1000 nm have been reported as important bands for predicting Mg, Zn, Mn and Fe in edible tree nuts (Bai et al., 2018). In addition, the model performance was closely related to the number of peaks in the 400–950 nm spectral range contained in the VIP curve. Compared to Ca ($r^2 = 0.70$), Mg ($r^2 = 0.74$), Mo ($r^2 = 0.82$) and Zn ($r^2 = 0.77$) model, the VIP curves for B ($r^2 = 0.28$), Fe ($r^2 = 0.34$) and Mn ($r^2 = 0.34$) models having poor prediction performance had more peaks. This phenomenon has also been observed in Ely et al. (2019).

5. Conclusion

The Ca, Mg, Mo and Zn nutrients in wheat kernel/flour were predicted at high credibility by combining the PSLR modeling and the VIS-NIR hyperspectral imaging. The prediction accuracy of the wheat kernel was higher than that of wheat flour. This study highlights the great potential for a rapid and non-destructive determination of micronutrients in kernels using hyperspectral images. These advances will provide opportunities for screening and breeding of high nutritional quality cereals, and can be widely applied to the assessment of cereal nutrition.

CRediT authorship contribution statement

Naiyue Hu: Conceptualization, Methodology, Formal analysis, Data curation, Writing - original draft, Writing - review & editing. **Wei Li:** Conceptualization, Methodology, Software, Writing - review & editing. **Chenghang Du:** Investigation. **Zhen Zhang:** Resources. **Yanmei Gao:** Resources. **Zhencai Sun:** Resources. **Li Yang:** Resources. **Kang Yu:** Writing - review & editing. **Yinghua Zhang:** Supervision, Funding acquisition. **Zhimin Wang:** Supervision, Funding acquisition.

Declaration of Competing Interest

The authors declare that they have no known competing financial interests or personal relationships that could have appeared to influence the work reported in this paper.

Acknowledgments

This work was supported by the National Key Research and Development Program of China (grant numbers: 2016YFD0300401, 2016YFD0300105), the National Natural Science Foundation of China (31871563), and the Earmarked Fund for Modern Agro-Industry Technology Research System (CARS-3). Financial support from the above sources is gratefully acknowledged.

Appendix A. Supplementary data

Supplementary data to this article can be found online at https://doi.org/10.1016/j.foodchem.2020.128473.

References

Alisaac, E., Behmann, J., Rathgeb, A., Karlovsky, P., Dehne, H. W., Mahlein, A. K. (2019). Assessment of Fusarium Infection and Mycotoxin Contamination of Wheat Kernels and Flour Using Hyperspectral Imaging. Toxins, 11, 556.

Atzberger, C., Guérif, M., Baret, F., & Werner, W. (2010). Comparative analysis of three chemometric techniques for the spectroradiometric assessment of canopy chlorophyll content in winter wheat. *Computers and Electronics in Agriculture, 73*(2), 165–173. https://doi.org/10.1016/j.compag.2010.05.006.

Bai, S. H., Tahmasbian, I., Zhou, J., Nevenimo, T., Hannet, G., Walton, D., Randall, B., Gama, T., & Wallace, H. M. (2018). A non-destructive determination of peroxide values, total nitrogen and mineral nutrients in an edible tree nut using hyperspectral imaging. *Computers and Electronics in Agriculture, 151*, 492–500. https://doi.org/10.1016/j.compag.2018.06.029.

Bouis, H. E., & Welch, R. M. (2010). Biofortification-a sustainable agricultural strategy for reducing micronutrient malnutrition in the global South. *Crop Science, 50*, S-20–S-32. https://doi.org/10.2135/cropsci2009.09.0531.

Brier, N. D., Gomand, S. V., Donner, E., Paterson, D., Delcour, J. A., Lombi, E., & Smolders, E. (2015). Distribution of minerals in wheat grains (Triticum aestivum L.) and in roller milling fractions affected by pearling. *Journal of Agricultural and Food Chemistry, 63*(4), 1276–1285.

Brier, N. D., Gomand, S. V., Donner, E., Paterson, D., Smolders, E., Delcour, J. A., & Lombi, E. (2016). Element distribution and iron speciation in mature wheat grains (*Triticum aestivum* L.) using synchrotron X-ray fluorescence microscopy mapping and X-ray absorption near-edge structure (XANES) imaging. *Plant, Cell & Environment, 39*(8), 1835–1847.

Cai, J. H. (2017). Near-infrared spectrum detection of wheat gluten protein content based on a combined filtering method. Journal of AOAC International, 100(5), 1565-1568.

Caporaso, N., Whitworth, M. B., & Fisk, I. D. (2018a). Protein content prediction in single wheat kernels using hyperspectral imaging. *Food Chemistry, 240*, 32–42. https://doi.org/10.1016/j.foodchem.2017.07.048.

Caporaso, N., Whitworth, M. B., & Fisk, I. D. (2018b). Near-Infrared spectroscopy and hyperspectral imaging for non-destructive quality assessment of cereal grains. *Applied Spectroscopy Reviews, 53*(8), 667–687. https://doi.org/10.1080/05704928.2018.1425214.

Coast, O., Shah, S., Ivakov, A., Gaju, O., Wilson, P. B., Posch, B. C., Bryant, C. J., Negrini, A. C. A., Evans, J. R., Condon, A. G., Silva-Pérez, V., Reynolds, M. P., Pogson, B. J., Millar, A. H., Furbank, R. T., & Atkin, O. K. (2019). Predicting dark respiration rates of wheat leaves from hyperspectral reflectance. *Plant, Cell and Environment, 42*(7), 2133–2150. https://doi.org/10.1111/pce.13544.

Delwiche, S. R., Graybosch, R. A., Amand, P. S., & Bai, G. (2011). Starch waxiness in hexaploid wheat (*Triticum aestivum* L.) by NIR reflectance spectroscopy. *Journal of Agricultural and Food Chemistry, 59*(8), 4002–4008. https://doi.org/10.1021/jf104528x.

Ely, K. S., Burnett, A. C., Lieberman-Cribbin, W., Serbin, S., Rogers, A. (2019). Spectroscopy can predict key leaf traits associated with source sink balance and carbon nitrogen status. Journal of Experimental Botany. doi: 10.1093/jxb/erz061 in press.

Gómez-Galera, S., Rojas, E., Sudhakar, D., Zhu, C., Pelacho, A. M., Capell, T., & Christou, P. (2010). Critical evaluation of strategies for mineral fortification of staple food crops. *Transgenic Research, 19*(2), 165–180. https://doi.org/10.1007/s11248-009-9311-y.

Gowen, A., Odonnell, C., Cullen, P., Downey, G., & Frias, J. (2007). Hyperspectral imaging – An emerging process analytical tool for food quality and safety control. *Trends in Food Science & Technology, 18*(12), 590–598. https://doi.org/10.1016/j.tifs.2007.06.001.

Hamnér, K., Weih, M., Eriksson, J., & Kirchmann, H. (2017). Influence of nitrogen supply on macro- and micronutrient accumulation during growth of winter wheat. *Field Crops Research, 213*, 118–129. https://doi.org/10.1016/j.fcr.2017.08.002.

Kuhn, M. (2015). Caret: Classification and regression training. *Astrophysics Source Code Library*.

Kumssa, D. B., Joy, E. J. M., Ander, E. L., Watts, M. J., Young, S. D., Walker, S., & Broadley, M. R. (2015). Dietary calcium and zinc deficiency risks are decreasing but remain prevalent. *Scientific Reports, 5*(1). https://doi.org/10.1038/srep10974.

Laborde, A., Jaillais, B., Bendoula, R., Roger, J.-M., Jouan-Rimbaud Bouveresse, D., Eveleigh, L., Bertrand, D., Boulanger, A., & Cordella, C. BY. (2020). A partial least squares-based approach to assess the light penetration depth in wheat flour by near infrared hyperspectral imaging. *Journal of Near Infrared Spectroscopy, 28*(1), 25–36. https://doi.org/10.1177/0967033519891594.

Liu, H. E., Wang, Q. Y., Rengel, Z., & Zhao, P. (2015). Zinc fertilization alters flour protein composition of winter wheat genotypes varying in gluten content. *Plant Soil and Environment, 61*(5), 195–200.

Liu, Z., Cai, W., & Shao, X. (2008). Outlier detection in near-infrared spectroscopic analysis by using Monte Carlo cross-validation. *Science in China Series B: Chemistry, 51*(8), 751–759. https://doi.org/10.1007/s11426-008-0080-x.

Mahesh, S., Jayas, D. S., Paliwal, J., & White, N. D. G. (2015). Comparison of partial least squares regression (PLSR) and principal components regression (PCR) methods for protein and hardness predictions using the near-infrared (nir) hyperspectral images of bulk samples of Canadian wheat. *Food and Bioprocess Technology, 8*(1), 31–40. https://doi.org/10.1007/s11947-014-1381-z.

Malmir, M., Tahmasbian, I., Xu, Z., Farrar, M. B., & Bai, S. H. (2019). Prediction of soil macro- and micro-elements in sieved and ground air-dried soils using laboratory-based hyperspectral imaging technique. *Geoderma, 340*, 70–80. https://doi.org/10.1016/j.geoderma.2018.12.049.

Manley, M. (2014). Near-infrared spectroscopy and hyperspectral imaging: Non-destructive analysis of biological materials. *Chemical Society Reviews, 43*(24), 8200–8214. https://doi.org/10.1039/C4CS00062E.

Pandey, P., Ge, Y., Stoerger, V., Schnable, J. C. (2017). High Throughput in vivo Analysis of Plant Leaf Chemical Properties Using Hyperspectral Imaging. Frontiers in Plant Science, 8.

Peiris, K. H. S., & Dowell, F. E. (2011). Determining weight and moisture properties of sound and *Fusarium*-damaged single wheat kernels by near-infrared spectroscopy. *Cereal Chemistry Journal, 88*(1), 45–50. https://doi.org/10.1094/CCHEM-04-10-0067.

Persson, D. P., Bang, T. C., Pedas, P. R., Kutman, U. B., Cakmak, I., Andersen, B., … Husted, S. (2016). Molecular speciation and tissue compartmentation of zinc in durum wheat grains with contrasting nutritional status. *New Phytologist, 211*(4), 1255–1265. https://doi.org/10.1111/nph.13989.

Rawat, N., Neelam, K., Tiwari, V. K., Dhaliwal, H. S., & Balyan, H. (2013). Biofortification of cereals to overcome hidden hunger. *Plant Breed*, n/a–n/a. https://doi.org/10.1111/pbr.12040.

Sendin, K., Williams, P. J., & Manley, M. (2017). Near infrared hyperspectral imaging in quality and safety evaluation of cereals. *Critical Reviews in Food Science and Nutrition, 58*, 575–590.

Shewry, P. R. (2009). Wheat. *Journal of Experimental Botany, 60*(6), 1537–1553. https://doi.org/10.1093/jxb/erp058.

Shi, H., Lei, Y., Louzada Prates, L., & Yu, P. (2019). Evaluation of near-infrared (NIR) and Fourier transform mid-infrared (ATR-FT/MIR) spectroscopy techniques combined with chemometrics for the determination of crude protein and intestinal protein digestibility of wheat. *Food Chemistry, 272*, 507–513. https://doi.org/10.1016/j.foodchem.2018.08.075.

Shiferaw, B., Smale, M., Braun, H. J., Duveiller, E., Reynolds, M., & Muricho, G. (2013). Crops that feed the world 10. Past successes and future challenges to the role played by wheat in global food security. *Food Security, 5*(3), 291–317.

Singh, C. B., Jayas, D. S., Paliwal, J., & White, N. D. G. (2009). Detection of insect-damaged wheat kernels using near-infrared hyperspectral imaging. *Journal of Stored Products Research, 45*(3), 151–158. https://doi.org/10.1016/j.jspr.2008.12.002.

Tamburini, E., Vincenzi, F., Costa, S., Mantovi, P., Pedrini, P., Castaldelli, G. (2017). Effects of Moisture and Particle Size on Quantitative Determination of Total Organic Carbon (TOC) in Soils Using Near-Infrared Spectroscopy. Sensors, 17, 2366.

Wiegmann, M., Backhaus, A., Seiffert, U., Thomas, W. T. B., Flavell, A. J., Pillen, K., Maurer, A. (2019). Optimizing the procedure of grain nutrient predictions in barley via hyperspectral imaging. PLOS ONE, 14, e0224491.

Wu, B., Andersch, F., Weschke, W., Weber, H., & Becker, J. S. (2013). Diverse accumulation and distribution of nutrient elements in developing wheat grain studied by laser ablation inductively coupled plasma mass spectrometry imaging. *Metallomics, 5*(9), 1276. https://doi.org/10.1039/c3mt00071k.

Wu, D.i., & Sun, D.-W. (2013). Advanced applications of hyperspectral imaging technology for food quality and safety analysis and assessment: A review — Part I: Fundamentals. *Innovative Food Science & Emerging Technologies, 19*, 1–14. https://doi.org/10.1016/j.ifset.2013.04.014.

Xing, J., Van Hung, P., Symons, S., Shahin, M., & Hatcher, D. (2009). Using a Short Wavelength Infrared (SWIR) hyperspectral imaging system to predict alpha amylase activity in individual Canadian western wheat kernels. *Sens. & Instrumen. Food Qual., 3*(4), 211–218. https://doi.org/10.1007/s11694-009-9087-z.

Zhang, Y., Song, Q., Yan, J., Tang, J., Zhao, R., Zhang, Y., … Ortiz-Monasterio, I. (2010). Mineral element concentrations in grains of Chinese wheat cultivars. *Euphytica, 174*(3), 303–313. https://doi.org/10.1007/s10681-009-0082-6.

Zheng, X., Peng, Y., Li, Y., Wang, W., Li, P. (2016). Non-destructive prediction of moisture of wheat seed kernel by using VIS/NIR hyperspectral technology. ASABE Paper No. 162461233. doi: 10.13031 / aim.20162461233.